Combination of ultra-micro angiography and sound touch elastography for diagnosis of primary Sjögren's syndrome: a diagnostic test

Zhikang Xu[1]^, Rumei Li[2]^, Bin Xia[2]^, Meijuan Jiang[1]^, Xiaojin Wu[1]^, Xuanxuan Zhang[2]^, Jianlian Pan[3]^, Jian Chen[2]^

[1]Zhejiang University School of Medicine, Hangzhou, China; [2]Department of Ultrasound Medicine, the Fourth Affiliated Hospital of Zhejiang University School of Medicine, Yiwu, China; [3]Department of Clinical and Research, Shenzhen Mindray Bio-Medical Electronics Co., Ltd., Shenzhen, China

Contributions: (I) Conception and design: Z Xu, J Chen; (II) Administrative support: J Chen; (III) Provision of study materials or patients: Z Xu, R Li; (IV) Collection and assembly of data: Z Xu, B Xia; (V) Data analysis and interpretation: Z Xu, M Jiang, X Wu; (VI) Manuscript writing: All authors; (VII) Final approval of manuscript: All authors.

Correspondence to: Jian Chen, MD. Department of Ultrasound Medicine, the Fourth Affiliated Hospital of Zhejiang University School of Medicine, N1 Shangcheng Avenue, Yiwu 322000, China. Email: chenjianzuj4h@zju.edu.cn.

Background: Primary Sjogren's syndrome (PSS) is a prevalent systemic autoimmune disease. However, the current gold standard diagnostic method is invasive, increasing the difficulty of patient acceptance and then delaying treatment. Therefore, a non-invasive, convenient, and effective diagnostic method is required. Although salivary gland ultrasonography (SGUS) is a good choice, previous studies have not found suitable parameters to diagnose PSS. Salivary gland involvement in patients with PSS leads to changes in gland stiffness and vascularization, so we combined sound touch elastography (STE) and ultra-microangiography (UMA) to demonstrate the diagnostic effectiveness of ultrasonography in PSS.

Methods: This prospective study included 27 patients with PSS and 20 healthy controls, with all participants forming a random series. Major salivary glands were examined with UMA and STE. Color pixel percentage (CPP), shear wave velocity (SWV), and Young's modulus values were investigated, and the combination of these parameters was evaluated by logistic regression analysis.

Results: For Young's modulus and SWV in the elasticity index, combined evaluation of both parotid glands and submandibular glands yielded an area under the receiver operating characteristic (ROC) curve (AUC) and confidence interval (CI) of 0.819, 0.699–0.938 and 0.801, 0.677–0.925, respectively. The levels of CPP in the parotid glands were significantly elevated (P<0.003) among patients compared to those in the control group, whereas the CPP values in the submandibular glands were not statistically different (P>0.086). We evaluated the elasticity values of the total 4 glands and the CPP of parotid glands together by logistic regression modeling. The ROC curve yielded an AUC of 0.954 (95% CI: specificity 0.849–0.994) which showed the best accuracy, with 92.6% sensitivity and 85.0% specificity.

Conclusions: The use of STE and UMA to examine the salivary glands may aid in the diagnosis of PSS, and their combination may be a promising method. This is good news for patients with PSS who are not suitable or unwilling to undergo labial gland biopsy.

^ ORCID: Zhikang Xu, 0000-0001-9385-3317; Rumei Li, 0000-0002-5083-2492; Bin Xia, 0000-0002-2061-4910; Meijuan Jiang, 0000-0003-3037-3791; Xiaojin Wu, 0000-0001-7469-4429; Xuanxuan Zhang, 0000-0001-6797-3489; Jianlian Pan, 0000-0002-5829-4641; Jian Chen, 0000-0003-2295-5505.

Introduction

Primary Sjögren's syndrome (PSS) is a prevalent systemic autoimmune disease with a 9:1 female-to-male prevalence and a peak incidence around the age of 50 (1). Lacrimal and salivary gland dysfunction are hallmarks of Sjögren's syndrome (SS), a common chronic autoimmune disease caused in part by lymphocytic infiltration and destruction of the gland parenchyma (2,3). Patients with PSS also frequently experience fatigue and joint pain, which significantly impact their quality of life and result in decreased productivity at work (4). In addition, patients with PSS are notably more likely than the general population to develop B-cell lymphoma—by a factor of 15 to 20 (5). Based on the latest official diagnostic criteria (6), biopsy of labial salivary glands is one of the most important diagnostic examinations. However, salivary gland biopsy is an invasive procedure that carries the risk of complications such as bleeding, pain, lip numbness, and infection (7). Therefore, the discovery of a non-invasive, convenient, and effective diagnostic method is particularly necessary.

Salivary gland ultrasonography (SGUS) as a straightforward, non-invasive method that is widely used to evaluate the involvement of salivary glands in PSS, including at the very early stages of the disease (8-10). In 2-dimensional (2D) grayscale ultrasound (US), many systems are used to evaluate the salivary gland echo structure (11,12). Although many of them have good diagnostic efficiency, as a kind of semi-quantitative index, they could not totally avoid the influence of the observer's subjectivity. Therefore, sonoelastography (SE) and power/color Doppler US with quantitative indicators have increasingly been given attention (13). Despite not being included in the current classification criteria, parotid ultrasonography was mentioned as a forthcoming diagnostic test in the most recent official diagnostic criteria for SGUS (6).

SE is a novel ultrasonographic technique for evaluating the stiffness of tissue. Sound touch elastography (STE) is a relatively new shear wave elastography (SWE) method that works with the diagnostic US device and utilizes ultra-wide beam tracking imaging technology. It effectively detects shear wave information up to 10 kHz per frame and provides real-time processing of signals. It eventually displays high-quality color-coded 2D tissue stiffness imaging and simultaneously provides quantitative measurement of a variety of elasticity indicators. Furthermore, it can automatically generate quality control histograms and assess movement stability, making the results more reliable. STE has shown good promise for detecting liver cirrhosis and differentiating benign and malignant thyroid nodules (14-16). Additionally, according to a recent study, parotid gland shear wave velocity (SWV) may be a useful parameter for diagnosing PSS (17); combining SWV values of parotid and submandibular glands achieved a sensitivity of 88.2% and specificity of 96.0% with an area under the receiver operating characteristic (ROC) curve (AUC) of 0.954 [95% confidence interval (CI): 0.893–0.986].

Recently, a neoteric ultra-microangiography (UMA) modality from Mindray Corporation (Shenzhen, China) was invented as a non-invasive method to demonstrate the blood supply within the region of interest (ROI). UMA has the same basic principle as traditional color Doppler flow imaging (CDFI). The biggest difference between the former is unfocused wave scanning and the spatiotemporal wall filtering algorithm, which can improve the quality of blood flow signals and improve the sensitivity of low-speed blood flow. UMA has 3 imaging modes: color UMA (CUMA) to show the blood flow speed information, corresponding to the traditional blood flow speed mode; power UMA (PUMA) to show the blood flow energy information, corresponding to the traditional blood flow energy mode; subtraction UMA (SUMA), UMA's unique display method, which has the highest sensitivity. Color pixel percentage (CPP) is a quantitative indicator of UMA used to evaluate blood flow sensitivity. A recent study demonstrated that it possesses the potential to serve as a noninvasive technique for diagnosing PSS (18), with an AUC of 0.906, and sensitivity and specificity rates of 87.5% and 72.5%, respectively.

Mononuclear cell infiltration and chronic inflammation of PSS results in the replacement of epithelial structure by fibrous tissue. This causes the gland to become stiffer and more blood supplied. Thus, there are many shortcomings to using STE or UMA alone to diagnose PSS. It is anticipated

7172

Xu et al. Ultrasonic multi-parameter combined diagnosis of PSS

that the integration of vascularity and stiffness data has the potential to enhance diagnostic accuracy. In this study, we aimed to evaluate the integrated diagnostic value of SGUS as a single PSS detection test. We evaluated 3 SGUS parameters' diagnostic accuracy: CPP, Young's modulus, and SWV. We present this article in accordance with the STARD reporting checklist (available at https://qims.amegroups.com/article/view/10.21037/qims-23-711/rc).

Methods

Patient population

Our study was designed prospectively. We randomly
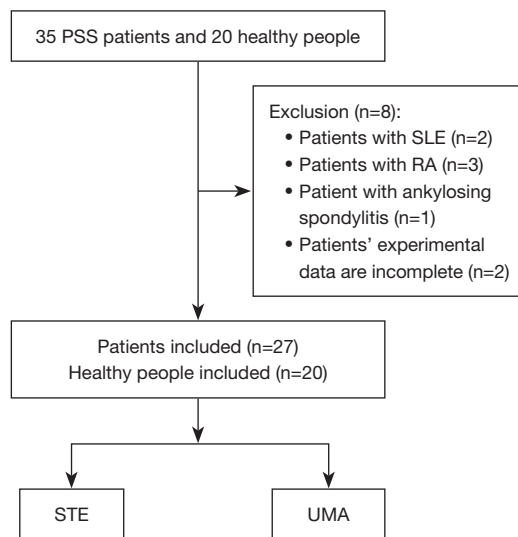
Figure 1 Flowchart illustrating the study process. PSS, primary Sjogren's syndrome; SLE, systemic lupus erythematosus; RA, rheumatoid arthritis; STE, sound touch elastography; UMA, ultra-microangiography.

selected 35 patients with PSS that had been diagnosed in the Fourth Affiliated Hospital of Zhejiang University School of Medicine by an experienced rheumatologist according to the American College of Rheumatology/European League Against Rheumatism (ACR/EULAR) 2016 criteria. Both SSA antibody tests and labial gland biopsies performed on these patients were positive. Labial gland biopsies were considered positive if the focus score (defined as the number of mononuclear infiltrates containing ≥ 50 lymphocytes/4 mm^2 of glandular tissue) was ≥ 1 (19). Further, patients with active hepatitis C virus infection, radiotherapy of the cervical spine, sarcoidosis, graft-versus-host disease, consumption of anticholinergic drugs, IgG4-related disease (6), rheumatic disease, and incomplete experimental data were not included (*Figure 1*). Simultaneously, a control group consisting of 20 individuals who were healthy and matched in terms of age and gender was included. The healthy participants had no medical history or physical examination abnormalities, did not exhibit any signs of dry mouth or eyes, did not have autoimmune diseases, sialadenitis, or mass lesions in their salivary glands, nor were they taking any medications. An experienced radiologist, who was not provided with any clinical details of the participants, conducted a uniform ultrasound examination on all individuals (35 patients and 20 controls) between December 1 and December 31, 2022. Meanwhile, we recorded their information, including height, weight, age, and medication history, as well as the duration of the disease (*Table 1*).

The Ethics Committee of the Fourth Affiliated Hospital of Zhejiang University School of Medicine (No. K2022187) approved this prospective study and informed consent was provided by all participants. The study was conducted in accordance with the Declaration of Helsinki (as revised in 2013).

Table 1 Characteristics information for the entire cohort

Parameters	PSS group (n=27)	Control group (n=20)	P value
Age (years)	53 (10.0)	53.9±5.8	>0.05
Sex (female), n (%)	25 (92.6)	20 (100.0)	>0.05
Sicca syndrome duration (years)	6±4.7	0	<0.01
Body mass index (kg/m^2)	24.0±2.5	23.4±2.7	>0.05
The maximum longitudinal section area of the parotid gland (cm^2)	12.8±2.1	11.2±2.9	0.05
The maximum longitudinal section area of the submandibular gland (cm^2)	3.5±0.8	3.2±0.8	<0.05

Normally distributed data are presented as mean ± standard deviation, non-normally distributed data are presented as median (interquartile range). PSS, primary Sjögren's syndrome.

Sonography technique

Both UMA and STE examinations were performed with a Resona 9 ultrasound system (Mindray Medical Solutions, Shenzhen, China) equipped with an L15-3WU phased array probe. Ultrasonography of the salivary glands mainly refers to examinations of the parotid and submandibular glands when the patients were in the supine position with the neck extended and the head turned to the other side. The parotid gland was thoroughly scanned in both longitudinal and transverse sections along the mandible; only longitudinal sections of the submandibular gland were scanned. The CPP and elasticity values were measured by an associate chief physician who was unaware of the diagnosis and laboratory test results. Patients were asked not to eat, drink, or exercise for 2 hours before the examinations.

Elasticity values measurement

To evaluate the stiffness of the glands quantitatively, elasticity values were taken from the longitudinal still images using dedicated software presenting in the scanner. First, switching to the shear wave mode, the probe was touched on the skin lightly. Next, the patients were instructed to hold their breath, and when the motion stability index at the top of the screen was green and the color-coded 2D tissue stiffness imaging remained constant for 3 seconds, the operator pressed the "update" button and the image was saved. At last, an oval region of interest (ROI) was selected on the most representative parts of both the parotid and submandibular glands, then SWV (Cs, m/s) and Young's modulus (E, kPa) were automatically calculated by the software. Measured data were taken only when the histogram at the bottom of the screen was approximately normally distributed (*Figure 2*). The average value of 3 measurements was taken as the final index.

CPP measurement

The longitudinal section of the parotid gland and the submandibular gland was also selected for the measurement of CPP (CPP = the ratio of colored pixels in a specific ROI). The observer took the picture and positioned the standard ROI, which was 20×5 mm^2, in the gland's center and computed the CPP automatically (*Figure 2*). Furthermore, it was crucial to steer clear of the typical major blood vessels found in the salivary gland, such as the external carotid artery and retromandibular vein in the parotid gland, as

well as the facial artery and vein in the submandibular gland. The same measurement protocol was used for CDFI, PUMA, and SUMA.

Statistical analysis

All statistical analyses were performed using the software packages SPSS 25.0 (IBM Corp., Armonk, NY, USA) and MedCalc 20.022 (MedCalc Software, Ostend, Belgium). For statistical comparisons, differences regarding median values were analyzed using Mann-Whitney *U* test whereas mean values were analyzed by Student's *t*-test. Categorical variables were evaluated using the Spearman square or Fisher exact chi-square test. The Shapiro-Wilk test was used to analyze the normality of data distribution. The ROC curve analysis and the Youden index were used to detect cut-off values for all indices. Logistic regression was employed to evaluate the diagnostic performance of combining STE and UMA in diagnosing PSS. By establishing a logistic regression equation, we could predict the probability of the patient's disease, the accuracy of which was evaluated by comparing it with the real disease situation, and the ROC curve was used to show the results. A P value of less than 0.05 was considered statistically significant. Normally distributed data are presented as mean ± standard deviation, non-normally distributed data are presented as median (interquartile range).

Results

The PSS group included 2 males and 25 females with a median age of 53 [10] years, and the mean time between labial gland biopsies and US imaging was 5 [6] years. The control group included 0 male and 20 females with a mean age of 53.9±5.8 years (*Table 1*). No statistically significant difference was observed between the patient and control cohorts with regards to age and gender (P>0.05). All the measured indicators were not significantly different between the right and left sides in both the patient and control groups (P>0.05).

SWV and Young's modulus had higher values both in the parotid and submandibular gland in the PSS group than in the controls (P<0.05). All these differences were statistically significant (*Table 2*). CPP, calculated in CDFI, PUMA, and SUMA modes, of both parotid glands and submandibular glands of the patients and controls group are presented in *Table 3*. In our study, the CPP values of CDFI, PUMA, and SUMA in parotid glands were remarkably higher in

7174

Xu et al. Ultrasonic multi-parameter combined diagnosis of PSS
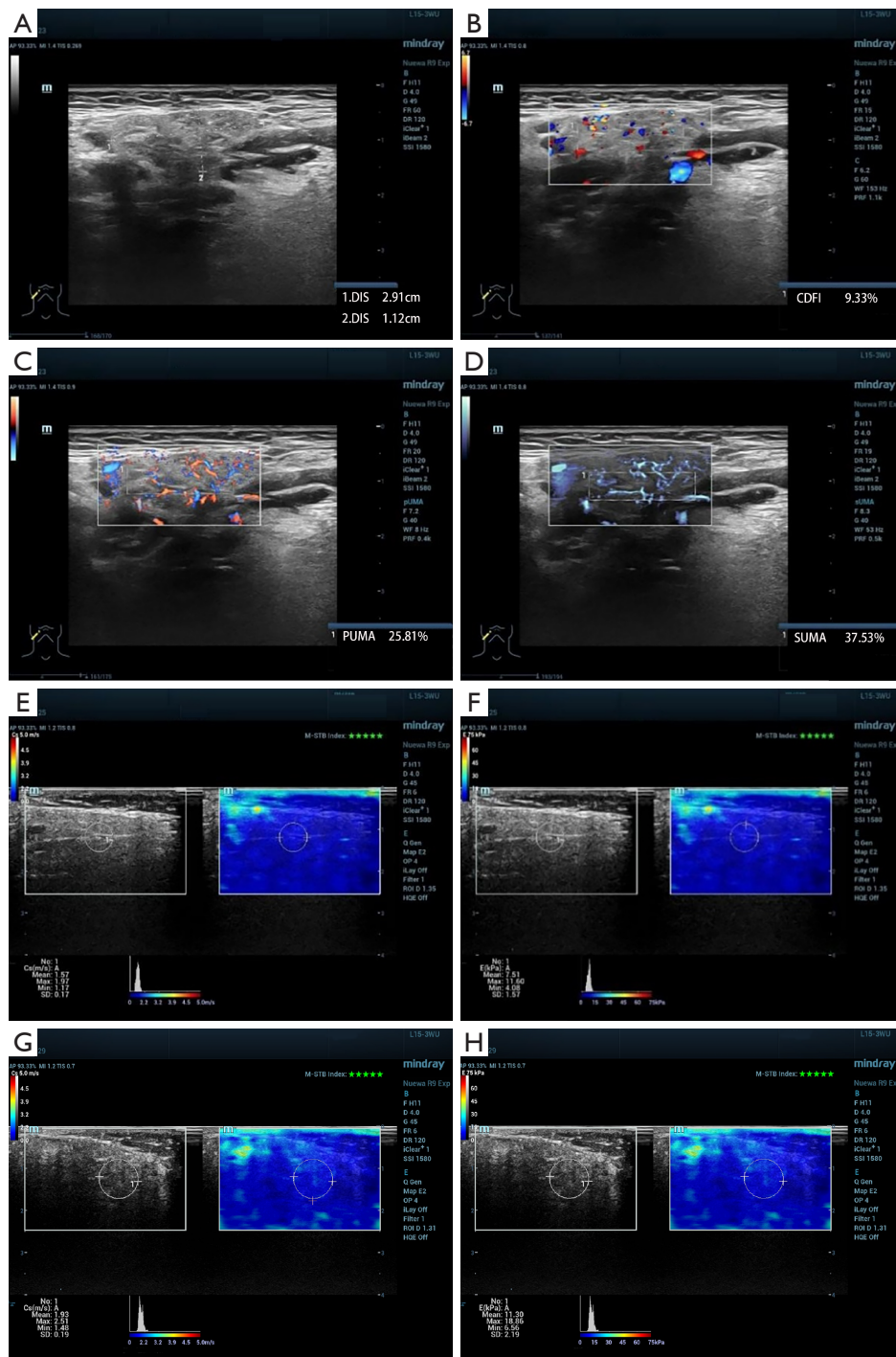
Figure 2 Examination of the submandibular gland in a woman with a history of Sjogren's syndrome of more than 10 years. (A) The B-mode image shows that the boundary between the involved submandibular gland and the surrounding tissue become blur. (B-D) The CPP of CDFI, PUMA, and SUMA are 9.33%, 25.81%, and 37.53%, respectively. (E,F) Images showing the parotid glands of a 52-year-old healthy woman. (G,H) Images showing the parotid glands of a 50-year-old woman with Sjogren's syndrome. Quantitative shear wave values (Cs mean: 1.57 m/s, E mean: 7.51 kPa; Cs mean: 1.93 m/s, E mean: 11.30 kPa) were measured by drawing an ROI on the B-mode image. DIS, distance; CDFI, color Doppler flow imaging; PUMA, power UMA; SUMA, subtraction UMA; UMA, ultra-microangiography; CPP, color pixel percentage; ROI, region of interest.

Table 2 Comparison between patients with PSS and the control group based on elasticity values

Parameters	PSS group (n=27)	Control group (n=20)	P value
SWV in PGs (m/s)	1.84±0.22	1.59±0.12	<0.001
Young's modulus in PGs (kPa)	10.65±2.76	7.77±1.16	<0.001
SWV in SGs (m/s)	1.93±0.19	1.77±0.10	0.006
Young's modulus in SGs (kPa)	11.48±2.21	9.59±1.03	0.004

Data are presented as mean ± standard deviation. SWV and Young's modulus for both PGs and SGs. PSS, primary Sjögren's syndrome; SWV, shear wave velocity; PGs, parotid glands; SGs, salivary glands.

Table 3 Comparison between patients with PSS and the control group based on CDFI, PUMA, and SUMA

Parameters	PSS group (n=27)	Control group (n=20)	P value
CDFI CPP in PGs	3.27±1.50	2.16±0.54	0.003
PUMA CPP in PGs	6.24 (2.78)	4.17±1.27	0.001
SUMA CPP in PGs	8.94±3.57	5.71±1.54	<0.001
CDFI CPP in SGs	5.72 (5.25)	4.46±1.56	0.519
PUMA CPP in SGs	11.46±5.64	9.19±3.20	0.086
SUMA CPP in SGs	16.80 (7.89)	13.01±4.10	0.197

Data are presented as mean ± standard deviation. CPP for both PGs and SGs. PSS, primary Sjögren's syndrome; CDFI, color Doppler flow imaging; PUMA, power ultra-microangiography; SUMA, subtraction ultra-microangiography; CPP, color pixel percentage; PGs, parotid glands; SGs, salivary glands.

the patient's group than in the control group (P=0.003, P=0.001, and P<0.001, respectively). On the contrary, the CPP values of CDFI, PUMA, and SUMA in submandibular glands were not statistically different (P=0.519, P=0.086, and P=0.197, respectively). *Figure 3* displays the ROC curve that was drawn based on different ultrasonic parameters for the diagnosis of PSS.

For Young's modulus in the elasticity index, combined evaluation of both parotid glands and submandibular glands [AUC: 0.819, 95% confidence interval (CI): 0.699–0.938] seemed to have better diagnostic accuracy than bilateral parotid glands (AUC: 0.802, 95% CI: 0.672–0.932) or submandibular glands (AUC: 0.680, 95% CI: 0.524–0.836) evaluation. Only the difference of AUC between the

submandibular gland and all 4 glands was statistically significant (P=0.017). The optimal Young's modulus cutoff value was 9.73, and the corresponding specificities and sensitivities were 90% and 66.7% (*Table 4*). The SWV also led to the same conclusion that combined evaluation of both parotid and submandibular glands (AUC: 0.801, 95% CI: 0.677–0.925) seemed to have better diagnostic accuracy than parotid (AUC: 0.799, 95% CI: 0.671–0.927) or submandibular glands (AUC: 0.674, 95% CI: 0.517–0.831) evaluation alone. However, only the difference of AUC between the submandibular gland and all 4 glands had statistical significance (P=0.024). The optimal SWV cutoff value was 1.80 for a total of 4 glands and the corresponding specificities and sensitivities were 90% and 63%, respectively.

The CDFI, PUMA, and SUMA CPP cut-off values for the diagnosis of PSS in the parotid gland that maximized the Youden index were 2.65, 6.31, and 7.46, respectively (AUC: 0.743, 95% CI: 0.599–0.886; AUC: 0.777, 95% CI: 0.646–0.907; AUC: 0.783, 95% CI: 0.653–0.913, respectively).

The SWV and Young's modulus values of all 4 glands and CPP of SUMA in parotid glands were statistically significant for the diagnosis of salivary gland involvement in PSS patients, therefore we evaluated them together by logistic regression modeling. The ROC curve yielded an AUC of 0.954 (95% CI: 0.849–0.994) which showed the best accuracy, with 92.6% sensitivity and 85.0% specificity.

Discussion

It is acknowledged that mononuclear cell infiltration of PSS autoimmune exocrinopathy tissue results in the replacement of epithelial structure by fibrous tissue as the disease progresses (20). Minor salivary gland biopsy with histopathologic confirmation of the disease remains the gold standard for PSS diagnosis. However, salivary gland sonography has recently gained prominence as a diagnostic tool (21). As a result, PSS patients could greatly benefit from the development of salivary gland diagnostic strategies that are both accurate and noninvasive. Our preliminary research demonstrates that STE and UMA may offer useful diagnostic data, and the absence of adverse events in this trial also demonstrates the safety of ultrasonography. To the best of our knowledge, no previous studies have combined SWV and CPP values in PSS diagnosis. In addition, our research is the first to examine the diagnostic accuracy of combining CPP and SWV values in PSS classification.

STE is a novel imaging technique that assesses tissue

7176

Xu et al. Ultrasonic multi-parameter combined diagnosis of PSS
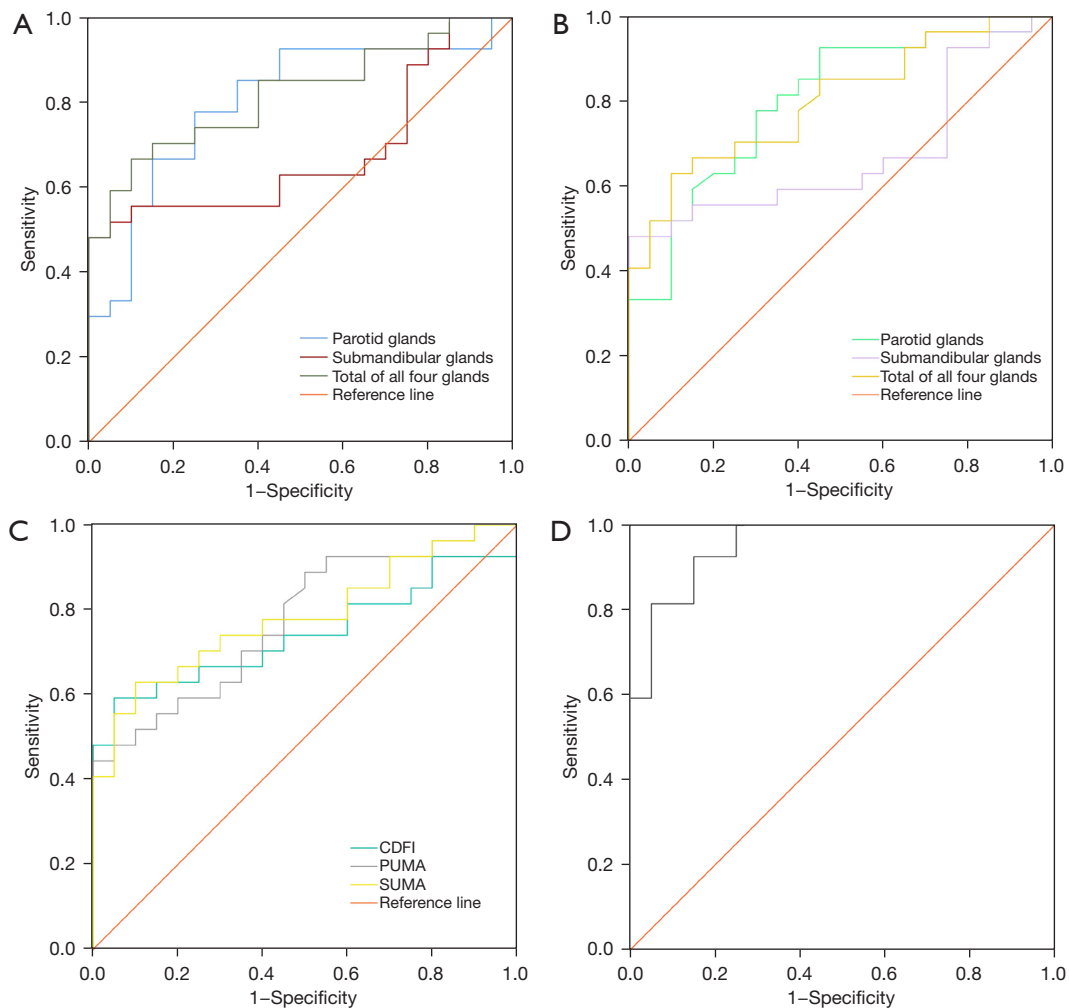
Figure 3 ROC curves of different parameters for diagnosing PSS. (A) AUCs of Young's modulus for diagnosing PSS. (B) AUCs of SWV for diagnosing PSS. (C) AUCs of UMA for diagnosing PSS in the parotid gland. (D) AUC of SWV and Young's modulus values of all 4 glands and CPP of SUMA in parotid glands for diagnosing PSS. CDFI, color Doppler flow imaging; PUMA, power ultra-microangiography; SUMA, subtraction ultra-microangiography; ROC, receiver operating characteristic; PSS, primary Sjögren's syndrome; AUC, area under the curve; SWV, shear wave velocity; UMA, ultra-microangiography; CPP, color pixel percentage.

stiffness in a noninvasive manner. It enables real-time 2D SWE imaging by capturing all shear wave data within the entire ROI simultaneously. Additionally, it can provide quantitative elastic parameters such as Cs and E concurrently. We found that a comprehensive evaluation of all 4 glands had the best diagnostic efficiency. It had a statistical difference with the diagnostic efficiency of the submandibular gland (P=0.024), but had no statistical difference compared with the diagnostic efficiency of the parotid gland (P=0.954). Although there was no significant difference in AUC between the parotid gland and the submandibular gland (P=0.132), the diagnostic efficiency of

the parotid gland seemed to be higher. A similar conclusion can be drawn from Oruk *et al.*'s study (22). It is probable that the dissimilar histological makeup of the parotid and submandibular glands accounts for this phenomenon. The parotid (and lacrimal) gland is primarily affected by PSS; the mixed submandibular gland is impaired to a lesser extent (23). Therefore, the differences in submandibular glands between PSS patients and healthy people are relatively small. We also observed that other studies (24,25) had reported that the mean SWV values for the salivary gland were 2.86 and 2.99 m/s, respectively, which were much higher than the values obtained in our study.

Table 4 Performance of different parameters

Parameters	Cut-off value	Sensitivity, %	Specificity, %	PPV, %	NPV, %	AUC (95% CI)	P
Parotid Young's modulus (kPa)	8.23	77.8	75.0	80.8	71.4	0.802 (0.672–0.932)	<0.001
Submandibular Young's modulus (kPa)	11.58	48.2	100.0	100.0	58.8	0.680 (0.524–0.836)	0.037
Young's modulus of 4 glands (kPa)	9.73	66.7	90.0	90.0	66.7	0.819 (0.699–0.938)	<0.001
Parotid SWV (m/s)	1.63	77.8	70.0	77.8	70.0	0.799 (0.671–0.927)	0.001
Submandibular SWV (m/s)	1.96	48.2	100.0	100.0	58.8	0.674 (0.517–0.831)	0.043
SWV of 4 glands (m/s)	1.80	63.0	90.0	89.5	64.3	0.801 (0.677–0.925)	<0.001
Parotid CPP of CDFI	2.65	59.0	95.0	94.1	63.3	0.743 (0.599–0.886)	0.005
Parotid CPP of PUMA	6.31	44.4	100.0	100.0	57.1	0.777 (0.646–0.907)	0.001
Parotid CPP of SUMA	7.46	63.0	90.0	89.5	64.3	0.783 (0.653–0.913)	0.001
Combined diagnostic index	0.44	92.6	85.0	89.3	89.5	0.954 (0.849–0.994)	<0.001

PPV, positive predictive value; NPV, negative predictive value; AUC, area under the receiver operating characteristic curve; CI, confidence interval; SWV, shear wave velocity; CPP, color pixel percentage; CDFI, color Doppler flow imaging; PUMA, power ultra-microangiography; SUMA, subtraction ultra-microangiography.

Consequently, the diagnostic performance and cutoff values were also different. These differences may be due to different sample sizes, control groups, and ultrasonic instruments.

UMA's developed late-model filtering and unfocused wave scanning methods successfully image small, slow-speed, vascular structures while removing background noise. UMA has a higher resolution and sensitivity than standard CDFI. In fact, in this study, UMA was found to be better than CDFI at identifying vascularity in salivary glands. In the parotid, CPP measured by various blood flow imaging methods had fair diagnostic performance (AUC: 0.743–0.783). Nevertheless, in the submandibular gland, there was no significant difference in CPP between the patient group and the control group, which may be due to the abundant blood supply already present in the submandibular gland. As a result, it makes blood flow changes resulting from PSS difficult to be detected.

The current investigation evaluated the diagnostic efficacy of distinct ultrasonographic imaging techniques (UMA and STE) both individually and in conjunction. No matter which gland was being evaluated, when UMA and STE were used together, the diagnostic performance was significantly better than when either was used alone (P<0.05).

This study has some limitations. The absence of an evaluation of inter- and intra-observer agreement is the first limitation, which indicates that the various parameters'

reliability was not sufficiently established. Additionally, it was a single-center study with small sample size. Consequently, the cutoff values for each parameter are not convincing. The usefulness of UMA and STE in the diagnosis of PSS will be better delineated in future via large-scale studies that analyze inter- and intra-observer repeatability.

Conclusions

The diagnostic efficacy of STE or UMA alone in detecting salivary gland involvement in patients with PSS is limited, but a combined evaluation, especially for the parotid glands or all 4 glands, may increase the diagnostic effectiveness of US for PSS. It has the potential to serve as a valuable non-intrusive tool in conjunction with clinical parameters, laboratory findings, and other US imaging techniques such as a 2D US scoring system and pixel analysis in elastic strain imaging for the diagnosis of PSS (26).

Acknowledgments

7178

Xu et al. Ultrasonic multi-parameter combined diagnosis of PSS

Footnote

Reporting Checklist: The authors have completed the STARD reporting checklist. Available at https://qims.amegroups. com/article/view/10.21037/qims-23-711/rc

Conflicts of Interest: All authors have completed the ICMJE uniform disclosure form (available at https://qims. amegroups.com/article/view/10.21037/qims-23-711/coif). JP states that he provides Shenzhen Mindray Bio-medical Electronics Co., Ltd. relevant technical consultation only when necessary. The other authors have no conflicts of interest to declare.

Ethical Statement: The authors are accountable for all aspects of the work in ensuring that questions related to the accuracy or integrity of any part of the work are appropriately investigated and resolved. The Ethics Committee of the Fourth Affiliated Hospital of Zhejiang University School of Medicine (No. K2022187) approved this prospective study and informed consent was provided by all participants. The study was conducted in accordance with the Declaration of Helsinki (as revised in 2013).

Open Access Statement: This is an Open Access article distributed in accordance with the Creative Commons Attribution-NonCommercial-NoDerivs 4.0 International License (CC BY-NC-ND 4.0), which permits the non-commercial replication and distribution of the article with the strict proviso that no changes or edits are made and the original work is properly cited (including links to both the formal publication through the relevant DOI and the license). See: https://creativecommons.org/licenses/by-nc-nd/4.0/.

References

1. Qin B, Wang J, Yang Z, Yang M, Ma N, Huang F, Zhong R. Epidemiology of primary Sjögren's syndrome: a systematic review and meta-analysis. Ann Rheum Dis 2015;74:1983-9.
2. Christodoulou MI, Kapsogeorgou EK, Moutsopoulos HM. Characteristics of the minor salivary gland infiltrates in Sjögren's syndrome. J Autoimmun 2010;34:400-7.
3. Tzioufas AG, Vlachoyiannopoulos PG. Sjogren's syndrome: an update on clinical, basic and diagnostic therapeutic aspects. J Autoimmun 2012;39:1-3.
4. Meijer JM, Meiners PM, Huddleston Slater JJ, Spijkervet FK, Kallenberg CG, Vissink A, Bootsma H. Health-related quality of life, employment and disability in patients with Sjogren's syndrome. Rheumatology (Oxford) 2009;48:1077-82.
5. Ramos-Casals M, Brito-Zerón P, Sisó-Almirall A, Bosch X. Primary Sjogren syndrome. BMJ 2012;344:e3821.
6. Shiboski CH, Shiboski SC, Seror R, Criswell LA, Labetoulle M, Lietman TM, Rasmussen A, Scofield H, Vitali C, Bowman SJ, Mariette X; . 2016 American College of Rheumatology/European League Against Rheumatism classification criteria for primary Sjögren's syndrome: A consensus and data-driven methodology involving three international patient cohorts. Ann Rheum Dis 2017;76:9-16.
7. Pellegrini M, Pulicari F, Zampetti P, Scribante A, Spadari F. Current Salivary Glands Biopsy Techniques: A Comprehensive Review. Healthcare (Basel) 2022.
8. Baldini C, Luciano N, Tarantini G, Pascale R, Sernissi F, Mosca M, Caramella D, Bombardieri S. Salivary gland ultrasonography: a highly specific tool for the early diagnosis of primary Sjögren's syndrome. Arthritis Res Ther 2015;17:146.
9. Delli K, Arends S, van Nimwegen JF, Dijkstra PU, Stel AJ, Spijkervet FKL, Bootsma H, Vissink A. Ultrasound of the Major Salivary Glands is a Reliable Imaging Technique in Patients with Clinically Suspected Primary Sjögren's Syndrome. Ultraschall Med 2018;39:328-33.
10. Mossel E, Delli K, van Nimwegen JF, Stel AJ, Kroese FGM, Spijkervet FKL, Vissink A, Arends S, Bootsma H; . Ultrasonography of major salivary glands compared with parotid and labial gland biopsy and classification criteria in patients with clinically suspected primary Sjögren's syndrome. Ann Rheum Dis 2017;76:1883-9.
11. Martel A, Coiffier G, Bleuzen A, Goasguen J, de Bandt M, Deligny C, Magnant J, Ferreira N, Diot E, Perdriger A, Maillot F. What is the best salivary gland ultrasonography scoring methods for the diagnosis of primary or secondary Sjögren's syndromes? Joint Bone Spine 2019;86:211-7.
12. Fana V, Dohn UM, Krabbe S, Terslev L. Application of the OMERACT Grey-scale Ultrasound Scoring System for salivary glands in a single-centre cohort of patients with suspected Sjögren's syndrome. RMD Open 2021;7:e001516.
13. Xu S, Luo J, Zhu C, Jiang J, Cheng H, Wang P, Hong J, Fang J, Pan J, Brown MA, Zhu X, Wang X. Performance Evaluation of Multiple Ultrasonographical Methods for the Detection of Primary Sjögren's Syndrome. Front Immunol 2021;12:777322.
14. Xiang H, Ling W, Ma L, Yang L, Lin T, Luo Y. Shear wave elastography using sound touch elastography

and supersonic shear imaging for liver measurements: a comparative study. Quant Imaging Med Surg 2022;12:2855-65.

15. Zhang L, Ding Z, Dong F, Wu H, Liang W, Tian H, Ye X, Luo H, Xu J. Diagnostic Performance of Multiple Sound Touch Elastography for Differentiating Benign and Malignant Thyroid Nodules. Front Pharmacol 2018;9:1359.

16. Zhang W, Wang J, Linghu R, Chen X, Dong C, Zhang S, et al. Comparison between spleen and liver stiffness measurements by sound touch elastography for diagnosing cirrhosis at different aminotransferase levels: a prospective multicenter study. Eur Radiol 2022;32:4980-90.

17. Chen S, Wang Y, Zhang G, Chen S. Combination of Salivary Gland Ultrasonography and Virtual Touch Quantification for Diagnosis of Sjögren's Syndrome: A Preliminary Study. Biomed Res Int 2016;2016:2793898.

18. Ustabaşıoğlu FE, Korkmaz S, İlgen U, Solak S, Kula O, Turan S, Emmüngil H. Quantitative Assessment of Salivary Gland Parenchymal Vascularization Using Power Doppler Ultrasound and Superb Microvascular Imaging: A Potential Tool in the Diagnosis of Sjögren's Syndrome. Balkan Med J 2020;37:203-7.

19. Pijpe J, Kalk WW, van der Wal JE, Vissink A, Kluin PM, Roodenburg JL, Bootsma H, Kallenberg CG, Spijkervet FK. Parotid gland biopsy compared with labial biopsy in the diagnosis of patients with primary Sjogren's syndrome. Rheumatology (Oxford) 2007;46:335-41.

20. Fox RI, Howell FV, Bone RC, Michelson P. Primary Sjogren syndrome: clinical and immunopathologic features. Semin Arthritis Rheum 1984;14:77-105.

21. Astorri E, Sutcliffe N, Richards PS, Suchak K, Pitzalis C, Bombardieri M, Tappuni AR. Ultrasound of the salivary glands is a strong predictor of labial gland biopsy histopathology in patients with sicca symptoms. J Oral Pathol Med 2016;45:450-4.

22. Oruk YE, Çildağ MB, Karaman CZ, Çildağ S. Effectiveness of ultrasonography and shear wave sonoelastography in Sjögren syndrome with salivary gland involvement. Ultrasonography 2021;40:584-93.

23. Dankof A, Morawietz L, Feist E. Labial salivary gland biopsy in Sjögren's syndrome. Pathologe 2006;27:416-21.

24. Hofauer B, Mansour N, Heiser C, Gahleitner C, Thuermel K, Bas M, Knopf A. Sonoelastographic Modalities in the Evaluation of Salivary Gland Characteristics in Sjögren's Syndrome. Ultrasound Med Biol 2016;42:2130-9.

25. Knopf A, Hofauer B, Thürmel K, Meier R, Stock K, Bas M, Manour N. Diagnostic utility of Acoustic Radiation Force Impulse (ARFI) imaging in primary Sjoegren`s syndrome. Eur Radiol 2015;25:3027-34.

26. Barbosa-Cobos RE, Torres-González R, Meza-Sánchez AV, Ventura-Ríos L, Concha-Del-Río LE, Ramírez-Bello J, Álvarez-Hernández E, Meléndez-Mercado CI, Enríquez-Sosa FE, Samuria-Flores CJ, Lugo-Zamudio GE, Hernández-Díaz C. A Novel Technique for the Evaluation and Interpretation of Elastography in Salivary Gland Involvement in Primary Sjögren Syndrome. Front Med (Lausanne) 2022;9:913589.